Available online at www.sciencedirect.com
ScienceDirect
International Journal of Mass Spectrometry 264 (2007) 164–174
International Journal of Mass Spectrometry
www.elsevier.com/locate/ijms

Gas phase FT ICR investigation of the production of phosphoranides and ion chemistry of tris(trifluoromethyl)phosphine

B. Kanawati [1], K.P. Wanczek *

Department of Physical and Inorganic Chemistry, University of Bremen, Bremen, Germany

Received 6 February 2007; received in revised form 7 April 2007; accepted 7 April 2007
Available online 12 April 2007

Abstract

In a long cylindrical ion cyclotron resonance (ICR) cell the ion chemistry of tris(trifluoromethyl)phosphine has been investigated. The only major negative primary ion, produced by dissociative electron attachment is the phosphide ion $(CF_3)_2P^-$, which reacts at elevated kinetic energy with the neutral molecules at 2×10^{-7} mbar to produce three phosphoranides: $CF_3PF_3^-$, $(CF_3)_2PF_2^-$, and $(CF_3)_3PF^-$. Simultaneously, three minor ions CF_3^-, F^-, and $C_2F_3^-$ are formed by self-collision-induced dissociation. Ion–molecule reactions between CF_3^- and $(CF_3)_3P$ have also been investigated. Positive ions form phosphonium ions and a diphosphonium product ion, $(CF_3)_2P–P(CF_3)_3^+$, whereas no P–P bond is observed with negative ions. All the structures and reaction pathways have been investigated theoretically with the aid of DFT calculations. The results are in excellent agreement with the experiments. The electron affinity of tris(trifluoromethyl)phosphine as EA($(CF_3)_3P$) = 22.6 kcal/mol has been calculated.

Keywords: FT ICR; Ion cyclotron resonance; Phosphoranide; CID; Ion–molecule reaction

1. Introduction

Tris(trifluoromethylphosphine) $(CF_3)_3P$ has been used as a ligand in metal coordination chemistry [1–5], where the σ donor and π acceptor capabilities of the phosphorous atom in this compound are involved. The effect of F and CF_3 substitution [6,7] on the σ donor properties of triarylphosphines toward forming complexes with different transition metals were also investigated.

Although several routes for the synthesis of $(CF_3)_3P$ were known in the condensed phase [8,9], Röschentaler and Shyshkov [10] have recently succeeded to get a high yield (>85%) of this compound in the condensed phase, starting from $(PhO)_3P$ and Me_3SiCF_3 at low temperatures.

The Lewis acidic character of $(CF_3)_3P$ has also been recently investigated by Kolomeisev et al. [11] by reacting $(CF_3)_3P$ with Me_4NF to give the phosphoranide $(CF_3)_3PF^-$ and by reacting $(CF_3)_3P$ with a mixture of Me_3SiCF_3 and Me_4NF to give another phosphoranide $(CF_3)_4P^-$ at low temperatures (−60 °C) in the condensed phase.

Although this first synthesis of the two phosphoranides has proved the Lewis acidity of $(CF_3)_3P$ toward high fluorinating agents such as Me_4NF and Me_3SiCF_3, it was not known whether there is a possibility of forming the phosphoranide ions $(CF_3)_3PF^-$ and $(CF_3)_4P^-$ in the gas phase due to ion–molecule reactions starting either from the phosphide ion $(CF_3)_2P^-$ or from CF_3^- and F^-, respectively. It is also interesting to gain insight in rearrangement processes that occur during formation of negative ions due to electron attachment. Such a rearrangement could produce new ions, which can undergo ion–molecule reactions with the neutrals at conditions of low pressure and in the absence of solvents in contrast to the conditions in the condensed phase. Additionally, oxidation of tricoordinated phosphines with a halogen, as well as deprotonation of a phosphorane with a P–H bond were well explained as synthetic routes to phosphoranides in the condensed phase [12].

Not much is known until now about the new class of tetracoordinated negative phosphorus ions. Although we have cited all the literature, which has come to our knowledge, it is clear that much work remains to be done in this field, in the gas phase and

* Corresponding author at: University of Bremen, NW2, A0090, D-28334 Bremen, Germany.
E-mail addresses: kanawati@t-online.de (B. Kanawati), icrwan@icr.uni-bremen.de (K.P. Wanczek).
[1] Present address: Max-Planck Institute for Chemistry – Atmospheric Chemistry Division, Joh.-Joachim Becherweg 27, 55128 Mainz, Germany.

1387-3806/$ – see front matter © 2007 Elsevier B.V. All rights reserved.
doi:10.1016/j.ijms.2007.04.008

in the condensed phase. This paper wants to present for the first time a detailed study of the gas phase ion chemistry of $(CF_3)_3P$ and the formation of phosphoranides in the gas phase.

To date, no investigations exist, which confirm the existence of CF_3 and F substituted phosphoranide ions in the gas phase. After a short discussion of the positive ion chemistry, the rich negative ion chemistry is discussed in detail. It is interesting to see whether a difference in the phosphoranide formation reaction exists between gas and condensed phase. How do phosphoranides fragment due to their acceleration in self-CID experiments? Can the nucleophilic character of CF_3^- towards $(CF_3)_3P$ be established in the gas phase?

2. Methods

2.1. Experimental

For the investigation a prototype FT ICR mass spectrometer Bruker 47X was employed, equipped with a 7 T superconducting magnet with 89 mm room temperature bore [13]. A simple UHV system with a gas inlet system yields a constant pressure of the compound. With a Varian VHS 600 diffusion pump and a liquid nitrogen cooled baffle a base pressure of 1.5×10^{-8} mbar was reached. The sample pressure was from 5×10^{-8} mbar to 8×10^{-6} mbar. Ion–molecule reactions and self-CID experiments were done at $(2 \pm 0.1) \times 10^{-7}$ mbar. This pressure gave optimum reaction yields.

Deviation from this pressure was chosen in some cases, to see whether phosphoranide formation is possible at lower pressure, to increase the resolution for accurate mass measurements, or to see if extremely high pressures in ICR are helpful to stabilize metastable ions through collisions with the neutral molecules. This is indicated in the text.

Positive ions were generated by electron impact. The negative ions were generated by dissociative attachment of low energy electrons, which are further decelerated by collisions with the neutral molecules. The electron kinetic energy was 0.2 eV for negative ions and 70 eV for positive ions. In the negative mode, the potential of the gate electrode was 0 V during the ionisation period and −50 V at all other times. For the generation of positive ions, the gate potentials were −60 V and −109 V, respectively.

Tris(trifluoromethyl)phosphine yields only one major negative ion species, the phosphide ion $(CF_3)_2P^-$ ($m/z = 169$) in this way, in addition to other minor ions, whose appearance is pressure and time dependent. Further details are directly included in Section 3.

A five section cylindrical ICR cell [14] closed by trapping electrodes was operated as a three section cell with long trapping tubes. Radius of the ICR cell is $r = 19$ mm. The length of the trapping electrodes is 56.6 mm. The detection and excitation electrode is 44.8 mm long. It has been kept at 0 V during all experiments. The trapping electrodes were at −3 V for negative ions and at +3 V for positive ions.

Before reaction, each ion species was isolated and all other ions were quenched. An acceleration scheme for the ions was used to generate reactions of kinetically excited ions or to dissociate selected ions collision-induced for structure elucidation purposes. With the excited ions, reactions can be observed in much larger abundances than with the thermal ions. Isolation and reaction of the ions has been performed with the aid of pulse experiments, described below.

The fragment ions obtained from self-CID experiments were also measured in high resolution mode to get accurate masses, so that a correct formula can be written, which helps to identify each fragment ion.

2.1.1. Pulse sequences

Acceleration processes for the experiments described in Section 3.

2.1.1.1. Pulse Sequence 1. With this pulse scheme the formation of the phosphide ion in addition to the phosphoranide ions $(CF_3)_2PF_2^-$ and $(CF_3)_3PF^-$ was studied as a function of pressure. The phosphide was allowed to grow for 1 s after the end of the ionisation pulse of 50 ms. A 100 ms quenching pulse was applied at the end of each pulse sequence.

2.1.1.2. Pulse Sequence 2. Electrons present in the ICR cell are a severe restriction in the study of negative ions.

The formation of $(CF_3)_2P^-$ by electron attachment is used to quench the electrons in the ICR cell in the following way:

$(CF_3)_2P^-$ was formed during 1 s after the end of an ionisation pulse of 100 ms duration and then radially quenched. After this reaction time, no new phosphide anions appear in the spectrum. This means that 1 s of reaction time is sufficient to deplete the trapped electrons completely. Therefore, $(CF_3)_2P^-$ was let to grow for 1 s after the end of the ionisation pulse and then accelerated radially for activation.

Phosphide activation after electron quenching gives three minor self-CID fragment ions F^-, $C_2F_3^-$, and CF_3^- in addition to high yields of the phosphoranides at $m/z = 157$, 207 and 257.

2.1.1.3. Pulse Sequence 3 for self-CID of secondary ions.

- Ionisation pulse 50 ms.
- 1 s growth time for $(CF_3)_2P^-$ (indirect electron depletion).
- Phosphide acceleration.
- Radial quench pulse for the primary ion and all secondary ions except the secondary ion that is under self-CID investigation.
- Acceleration of the isolated secondary ion for activation.
- Variable delay time.
- Radial dipolar excitation for ion detection.

2.1.1.4. Pulse Sequence 4 for the ion–molecule reactions of CF_3^-.

- Ionisation pulse 50 ms.
- 1 s growth time for $(CF_3)_2P^-$ (electron depletion).
- Phosphide acceleration.
- Radial quench pulse for $m/z = 19$, 81, 157, 169, 207, and 257.
- Variable delay time.
- Radial dipolar excitation for ion detection.

2.2. Calculations

SIMION [15] simulations have shown that the ion motion in the negative potential well used in the experiment is not confined to the central region of the ICR-cell, where detection and excitation are applied. The ions are also trapped inside the trapping electrodes too. A few ions drift into the central region by collisional damping in a few milliseconds. However, no increase in relative total ion current (TIC, defined as the sum of all relative ion intensities) as a function of time was observed during all time-dependent investigations described here. At this potential configuration and a pressure of 2×10^{-7} mbar ions can be trapped for 28 s without any loss.

DFT calculations were done using Gaussian 03 W [16]. For geometry optimization and frequency analysis the B3LYP method with 6-31 + G(d) basis set was employed. Single point energy calculations were done on those optimized geometries using B3LYP and a higher basis set 6-311 + G(2d). Diffuse functions are necessary especially for ions to describe their structures correctly. Every wave function used in geometry optimization and frequency analysis was previously tested by running stability tests to ensure that the wave function does represent the lowest energy solution to the SCF equations.

3. Results and discussion

In the following, a short discussion of the positive ion chemistry is given. Formation reactions of the phosphoranide ions will then be presented in detail. Then the ion–molecule reactions of the ions formed by collision-induced dissociation (self-CID) will be discussed. Structure elucidation of the product ions using self-CID is the next part of the paper. Finally, the absence of the phosphoranide ion $(CF_3)_4P^-$ during the reaction between CF_3^- and the neutrals will be explained.

3.1. Positive ions

In the ICR primary ion spectrum, the molecular ion ($m/z = 238$) as well as the following fragment ions are observed:

$(CF_3)_2P{=}CF_2^+ (m/z = 219)$, $F_3CP{=}CF_2^{\bullet +} (m/z = 150)$,

$F_2C{=}P{=}CF_2^+ (m/z = 131)$, $CF_2{=}PF^{\bullet +} (m/z = 100)$,

$CF_3^+ (m/z = 69)$ and $PF_2^+ (m/z = 69)$.

Investigations [17] at variable pressures and reaction times with all positive ions of $(CF_3)_3P$ have indicated that CF_3^+ ($m/z = 69$) is very reactive. It reacts with the neutral molecules to two phosphonium ions $F_2C{=}P{=}CF_2^+$ ($m/z = 131$) and $(CF_3)_2P{=}CF_2^+$ ($m/z = 219$). Both ions are also formed as primary ions. The latter ion reacts in an electrophilic reaction with $(CF_3)_3P$, a product ion with a P–P bond is formed, $(CF_3)_2P{-}P(CF_3)_3^+$ ($m/z = 407$). This fact illustrates the nucleophilic reactivity of $(CF_3)_3P$ towards the phosphonium ion $(CF_3)_2P{=}CF_2^+$. $(CF_3)_2P{-}P(CF_3)_3^+$ is formed only in low abundance, because the CF_3 substituents in $(CF_3)_3P$ weaken the nucleophilicity of the phosphorous atom.

3.2. Negative ions

3.2.1. Pressure dependence of negative ion spectra

At a pressure of 5×10^{-8} mbar and without delay time, only one primary ion appears in the negative mode $m/z = 169$. No additional primary ions were observed at this pressure if a delay time of 1 s was allowed, during which dissociative electron attachment took place. High resolution spectra of this ion indicate the formula C_2F_6P. The same is true at 1×10^{-7} mbar. In the condensed phase, several efforts were applied to stabilize the phosphide as a salt and to see whether hyperconjucation is feasible [18,19].

At a higher pressure of 2×10^{-7} mbar and without delay time after ionisation, two primary ions were observed in ICR. $m/z = 169$ appears as a basis peak and $m/z = 81$ builds a relative signal intensity of 3.3% only. After a delay time of 1 s, two additional ions were observed $m/z = 207$, 0.7%, $m/z = 257$, 0.8%. Accurate mass measurements for these additional ions indicated the formulae $C_2F_8P^-$ for $m/z = 207$ and $C_3F_{10}P^-$ for $m/z = 257$. These high resolution measurements exclude the possibility for formation of ions, which have P–P bonds such as $CF_7P_2^-$ for $m/z = 207$ and $C_2F_9P_2^-$ for $m/z = 257$.

The differences between theoretical and measured m/z are relatively high, due to the high pressure of 2×10^{-7} mbar, necessary to form the ions. But for determination of the precise masses of the small molecules studied here, the precision is sufficient.

Accurate mass measurement for the primary ion $m/z = 81$, obtained at 2×10^{-7} mbar indicated the formula $C_2F_3^-$ und thus excludes the possibility of P_2F^- formation. $C_2F_3^-$ has a C–C bond which does not exist in $(CF_3)_3P$. This observation leads us to presume that a rearrangement of the metastable excited phosphine anion $(CF_3)_3P^{-*}$ occurs, which leads to the observed $C_2F_3^-$.

We were also interested to know how much internal energy does the neutral molecule gain during the thermal electron attachment. So we have run DFT calculations by optimizing first the following structures in Fig. 2 using the B3LYB/6-31 + G(d) method and basis set, then run a frequency analysis with the same method and basis set, to obtain the zero point vibrational energy. Finally a single point energy calculation for each structure has been done using B3LYP/6-311 + G(2d) to determine the

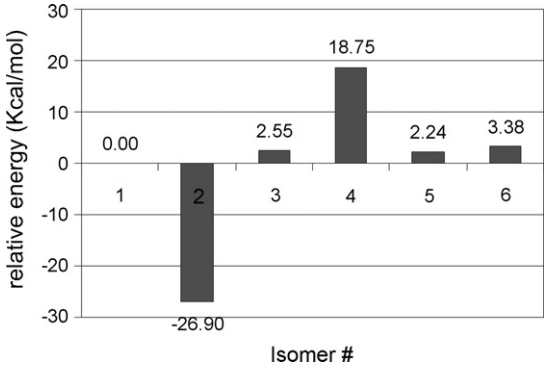

Fig. 1. Calculated zero-point energies of the six isomers of $C_2F_6P^-$ shown in Fig. 2, relative to the phosphide ion.

total electronic energy at 0 K. $(CF_3)_3P$ has an electron affinity of EA($(CF_3)_3P$) = 22.6 kcal/mol.

$(CF_3)_3P^-$* ions were not observed in the negative mode in the pressure range from 5×10^{-8} to 6×10^{-6} mbar. To determine an upper limit of the lifetime of this excited anion we applied a radial quench pulse at $m/z = 238$ to quench $(CF_3)_3P^-$* during the whole experimental events from the start of ionisation pulse until detection. The ion $(CF_3)_2P^-$ was not affected by this quench pulse. This means that the excited $(CF_3)_3P^-$* ion has a life time shorter than 62.9 μs, which is the time needed for an ion at thermal cyclotron radius to reach the ring electrodes of the ICR cell at the experimental conditions listed in the experimental section. The ejection of the non-observed radical anion of tris(trifluoromethyl)phosphine is similar to an ejection ICR experiment reported previously by Kleingeld and Nibbering [20].

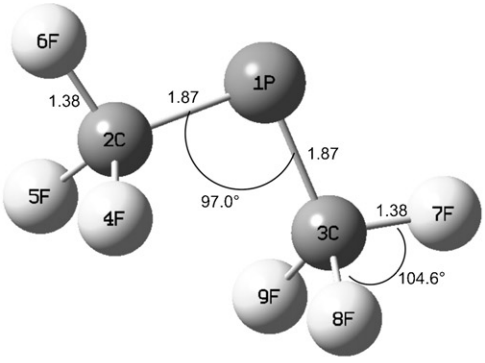

169-i1

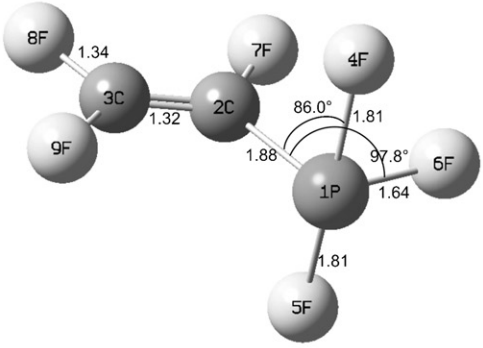

169-i2

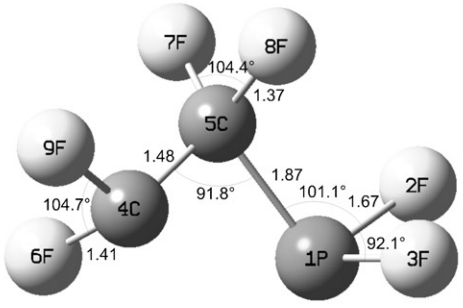

169-i3

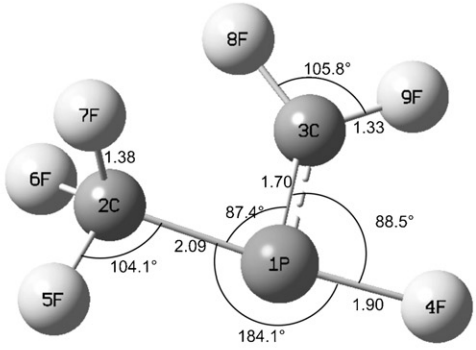

169-i4

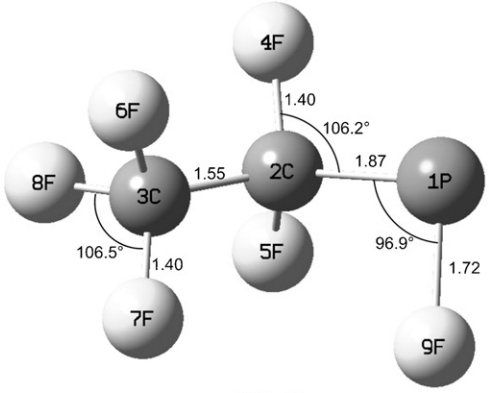

169-i5

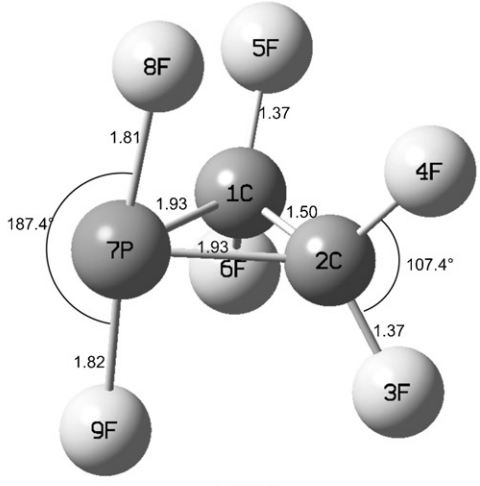

169-i6

Fig. 2. Optimized structures for isomer anions at $m/z = 169$.

There are six possible isomers of the anion with the sum formula $C_2F_6P^-$. The energies of these structures relative to $(CF_3)_2P^-$ are shown in Fig. 1. The corresponding optimized structures of these six isomer anions are shown in Fig. 2.

Eq. (1) illustrates the decomposition of the excited anion $(CF_3)_3P^-$* to yield the phosphide anion $(CF_3)_2P^-$ ($m/z = 169$) and a CF_3 radical, as calculated with DFT. The overall reaction is endothermic by 16.5 kcal/mol at 0 K and 15.6 kcal/mol at 298 K. Since the electron affinity of $(CF_3)_2P$ (66.1 kcal/mol) is by 22.8 kcal/mol higher than the electron affinity of CF_3 (43.3 kcal/mol), $(CF_3)_2P^-$ builds the basis peak as a primary ion in the mass spectrum and no primary CF_3^- has been found.

The observed primary ion $m/z = 81$ with the sum formula of $C_2F_3^-$ may be obtained from one or more of the following isomers: 169-i2, 169-i3, 169-i5, and 169-i6. Although three of these isomers have higher energies relative to the phosphide anion, these energies may be obtained from the high electron affinity of $(CF_3)_3P$, which can induce rearrangement in the excited $(CF_3)_3P^-$*.

From DFT calculations, no transition state could be found for the rearrangement of 169-i1 to 169-i5 or to 169-i6. Such a transition state may explain the observation of $C_2F_3^-$ as a primary ion in the mass spectrum. In addition, hyperconjucation (Eq. (2)) of the phosphide anion $(CF_3)_2P^-$ ($m/z = 169$) to CF_2=P(F)CF_3 (169-i4) anion is endothermic by 18.8 kcal/mol at 0 K and by 19.2 kcal/mol at 298 K with a high activation energy of 36.9 kcal/mol at 0 K and 37.1 at 298 K. The formation of $C_2F_3^-$ remains unexplained.

3.2.2. Acceleration of the primary ion m/z = 169

Without acceleration, the phosphide ion $(CF_3)_2P^-$ ($m/z = 169$) is totally inert in the pressure range from 1×10^{-7} to 6×10^{-6} mbar regardless of whatever reaction time is allowed between the end of the ionisation pulse and detection. Acceleration of this ion with a radial excitation pulse of 10 μs and P–P voltage of 53 V yields large signal intensities of $m/z = 207$ and $m/z = 257$ after 1 s reaction time at 2×10^{-7} mbar (Fig. 3).

At low pressures such as 5×10^{-8} mbar, no ion at $m/z = 257$ has been observed. Ion $m/z = 207$ was observed in a minor signal intensity after the same delay time of 1 s after $m/z = 169$ acceleration.

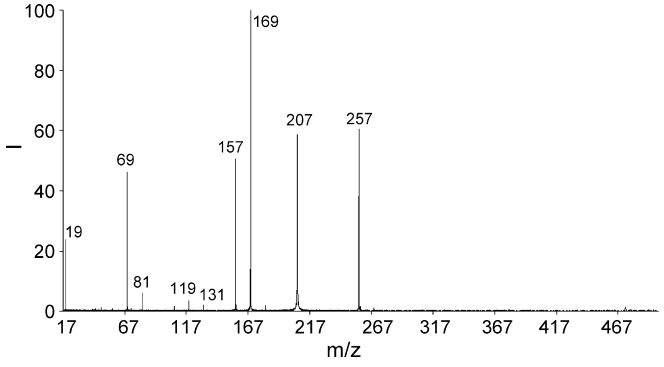

Fig. 3. Negative mode mass spectrum after primary ion $m/z = 169$ acceleration with a reaction time of 1 s at 2×10^{-7} mbar.

We found that these experimental conditions of pressure and reaction time after acceleration are ideal to obtain a high yield of the secondary ions. High resolution mass spectra indicate that all three major secondary ions with $m/z = 157$, 207, and 257 do not contain P–P bonds. We assume that these secondary ions correspond to the following phosphoranides: $CF_3PF_3^-$ ($m/z = 157$), $(CF_3)_2PF_2^-$ ($m/z = 207$), and $(CF_3)_3PF^-$ ($m/z = 257$). Evidence for these assumptions is provided from the self-CID-experiments presented in the next section.

3.2.3. Self-CID of the secondary ions

Fragmentation of the secondary ion $m/z = 257$ (after radial acceleration with a pulse of 10 μs duration 53 V_{p-p} at 2×10^{-7} mbar) produces product ions with the sum formulae CF_3^-, CPF_6^- and $C_2F_8P^-$. These sum formulae were verified by experiments performed in the high resolution mode.

Eqs. (3.1–3.4) summarize the reaction pathways. The reaction energies have been calculated by DFT.

It is interesting to see, that pathways, which involve rearrangements (Eqs. (3.1–3.4)) (Scheme 1) have lower energy demands than the other pathways, where only chemical bonds are broken. The fragment ion $(CF_3)_2P^-$ ($m/z = 169$) originates from $(CF_3)_3P$, but CF_3^- ($m/z = 69$) can not originate from the neutral molecule because the electron affinity of the phosphide is higher than that of CF_3 as we have explicitly indicated from our DFT calculations above.

Fragmentation of the secondary ion $m/z = 207$ (after radial acceleration with a pulse of 10 μs duration 53 V_{p-p} at 2×10^{-7} mbar) yields anions CF_3^- ($m/z = 69$) and CPF_6^- ($m/z = 157$).

We notice that rearrangement (Eq. (4.2)) (Scheme 2) is energetically favourable and even less endothermic than simple bond breaking as in Eq. (4.1).

No fragment ion with $m/z = 169$ has been observed for the secondary ion $m/z = 207$ in the CID experiments, contrary to $m/z = 257$. Therefore, it is assumed that the ion $(CF_3)_2P^-$ ($m/z = 169$) formed in self-CID experiments, originates from the ion $m/z = 257$ and not from the neutral phosphane.

Fragmentation of the secondary ion $m/z = 157$ (after radial acceleration with a pulse of 10 μs duration 53 V_{p-p} at 2×10^{-7} mbar) gives CF_3^- ($m/z = 69$) and $C_3F_{10}P^-$ $m/z = 257$ Scheme 3.

The secondary ion $m/z = 157$ is more stable toward fragmentation in comparison with the other secondary ions discussed above, since no fragment ions were observed after 100 ms delay time upon acceleration. The spectrum obtained after 500 ms contains two ions with small relative signal intensities, $m/z = 69$ and $m/z = 257$. Ion $m/z = 257$ is a product ion of an ion–molecule reaction. The sum formulae of the two product ions have been confirmed with high resolution acquisitions.

Eq. (5.3) shows the energy requirement for fragmentation of ion $m/z = 157$. CF_3^- and PF_3; not PF_3^- and CF_3 are formed, because the calculated electron affinity of CF_3 (43.3 kcal/mol) is higher than that of PF_3 (5.4 kcal/mol). The formation of CF_3^- rather than PF_3^- has been proved in this experiment.

When the duration of the radial acceleration pulse is increased from 10 to 30 μs, no fragment ions are observed till a delay time

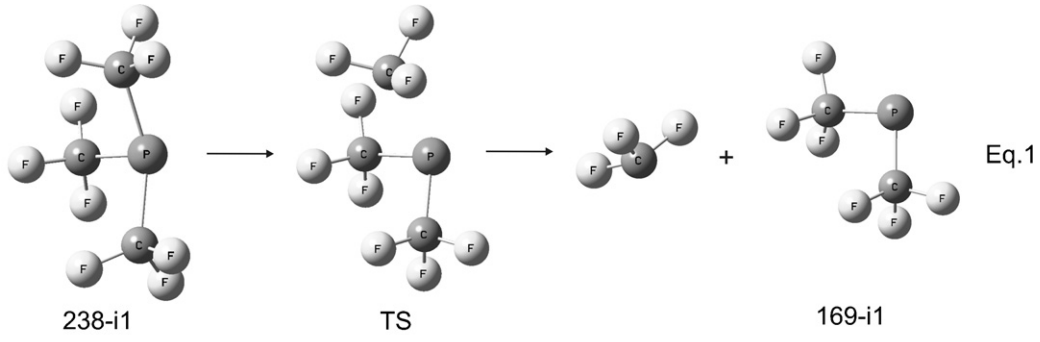

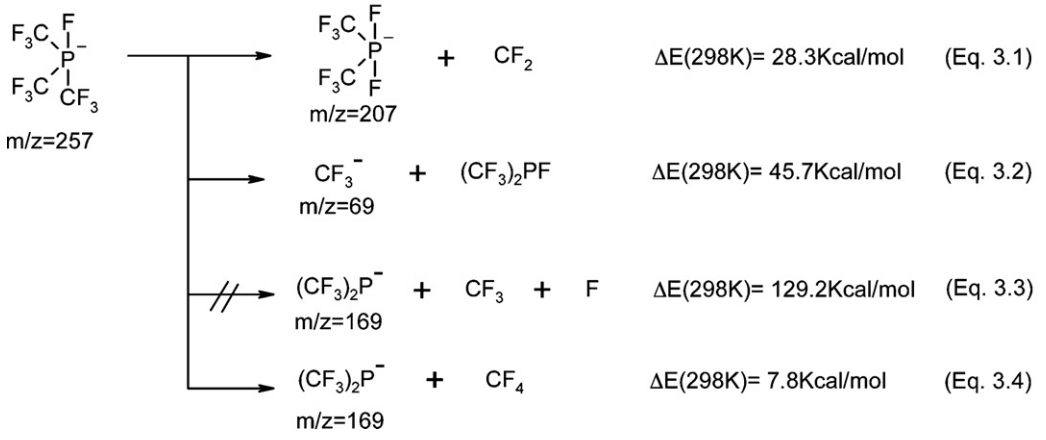

Scheme 1. Fragmentation pathways for ion $m/z = 257$ in the gas phase.

of 100 ms. After 500 ms delay time and the longer acceleration pulse, the same two signals $m/z = 69$ and $m/z = 257$ appear again. The signal intensity of CF_3^- has increased to 17.7% relative to the base peak of $m/z = 157$. The signal intensity of the product ion $m/z = 257$ is unchanged in comparison with that of $m/z = 257$ after acceleration period of only 10us and delay time of 500 ms.

This result reinforces the assumption, that the observed CF_3^- is a fragment ion and not a result of ion–molecule reaction because the signal intensity of this ion increases as the radial acceleration pulse for $m/z = 157$ increases. The signal intensity of $m/z = 257$ is independent of the radial acceleration pulse. It is dependent on the delay time after acceleration and this is characteristic for a product ion formed as a result of an ion–molecule reaction.

We will return to this problem again after we finish the discussion of the thermal ion–molecule reactions between CF_3^- and

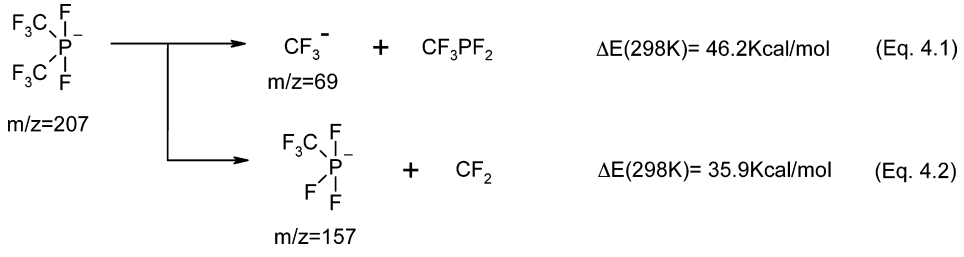

Scheme 2. Fragmentation pathways for ion $m/z = 207$ in the gas phase.

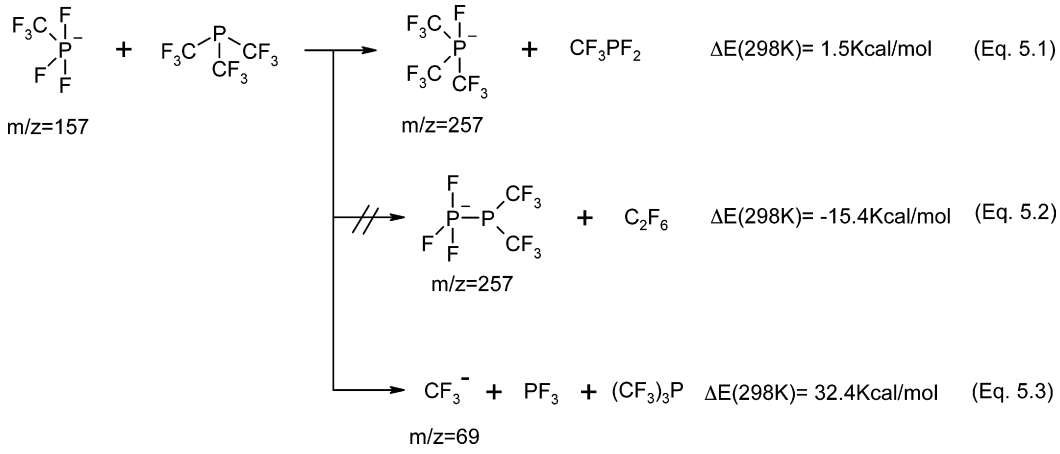

Scheme 3. Fragmentation pathways for ion $m/z = 157$ in the gas phase.

$(CF_3)_3P$, because it contains valuable information, which proves the formation of the phosphoranide $(CF_3)_3PF^-$ ($m/z = 257$) as a quaternary product ion from the tertiary product ion $CF_3PF_3^-$ ($m/z = 157$).

From the sum formulae obtained from high resolution experiments and the fragmentation pattern for each secondary ion obtained as a result of acceleration of the primary ion $m/z = 169$ one obtains for the ions $m/z = 257$, 207, 157, 81, 69, 19 the formulae $(CF_3)_3PF^-$, $(CF_3)_2PF_2^-$, $CF_3PF_3^-$, $C_2F_3^-$, CF_3^-, F^-, respectively.

Thus, we confirm the existence of the phosphoranides $(CF_3)_3PF^-$, $(CF_3)_2PF_2^-$, and $CF_3PF_3^-$ in the gas phase and we confirm that their formations have high energy barriers, which could be overcome experimentally by radial acceleration of the primary phosphide ion ($m/z = 169$) in the ICR cell at the experimental conditions discussed above.

It is at this point interesting to know whether thermal pathways exist to yield the same phosphoranides, which are formed in the acceleration experiment discussed above. The ion–molecule reaction between the isolated CF_3^- secondary ion and the neutral molecules at 2×10^{-7} mbar is discussed in Section 3.2.5.

3.2.4. Electron affinities of multiply charged ions of $(CF_3)_2P$

Accelerating the primary phosphide ion $m/z = 169$ at 2×10^{-7} mbar with a radial acceleration pulse of 10 μs without assigning additional delay times produces two signals $m/z = 84.475$ and $m/z = 56.320$, which are harmonics of the resonance frequency of the ion $m/z = 169$. To exclude the possibility of formation of multiply charged ions, DFT calculations have been done.

Multiply charged anions of $(CF_3)_2P$ have large negative electron affinities of -35.8 kcal/mol and −199.7 kcal/mol for $(CF_3)_2P^{2-}$ and $(CF_3)_2P^{3-}$, respectively. Thus a second or third electron attachment to $(CF_3)_2P^-$ moiety is highly endothermic and cannot be observed at the experimental conditions discussed in Section 2.1. The signals $m/z = 84.475$ and $m/z = 56.320$ represents the second and the third harmonics, respectively.

Fig. 4 lists the DFT structures of the fragments $(CF_3)_2P$, $(CF_3)_2P^-$, $(CF_3)_2P^{2-}$ and $(CF_3)_2P^{3-}$. The C–P–C angle increases slightly from $(CF_3)_2P^-$ to $(CF_3)_2P^{3-}$, while the P–C bond length in all the anions is the same.

3.2.5. Ion–molecule reaction between CF_3^- and $(CF_3)_3P$

To see whether $(CF_3)_4P^-$ or the lower mass phosphoranides $(CF_3)_3PF^-$ ($m/z = 257$), $(CF_3)_2PF_2^-$ ($m/z = 207$), $CF_3PF_3^-$ ($m/z = 157$) can be formed as a result of an ion–molecule reaction between CF_3^- and $(CF_3)_3P$, the secondary ion CF_3^- has been isolated (after 1 s reaction time between the accelerated primary phosphide ion $(CF_3)_2P^-$ and the neutrals). The m/z values of all product ions were measured in high resolution mode at all the reaction times utilized. No dependence of accurate mass upon reaction time was observed, as expected. Variable delay times between 0 and 5 s were assigned to trace the behaviour of absolute signal intensities of all ions, which contribute to the reaction (Fig. 5).

From Fig. 5, we notice two reactive ions: the secondary CF_3^- ion and the tertiary ion $m/z = 157$ which appears in minor signal intensity along the reaction time investigated. From this figure alone, it is not obvious whether high m/z ions such as $m/z = 169$, 207 and 257 are directly produced from CF_3^- ion–molecule reaction or from the reactive tertiary ion $m/z = 157$, that might contribute to the production of any other higher m/z ions.

Although $m/z = 157$ has a small absolute signal intensity, as a reaction intermediate, it may yield high amounts of other product ions.

The tertiary ion $m/z = 157$ has been quenched using a radial quench pulse of 53 V_{p-p} with the same duration as the reaction time. If this ion is quenched (Fig. 6), the product ion $m/z = 169$ does not appear. So it is now clear that the tertiary ion $m/z = 157$ is responsible for formation of ion $m/z = 169$. We can also conclude that the product ions $m/z = 207$ and $m/z = 257$ are formed directly from CF_3^- ion–molecule reaction. The mechanisms of the formation of the product ions $m/z = 169$, 207 and 257 are established by ejection experiments.

3.2.5.1. Mechanism and energy balance of the ion–molecule reaction $CF_3^- + (CF_3)_3P$. DFT calculations have indicated that

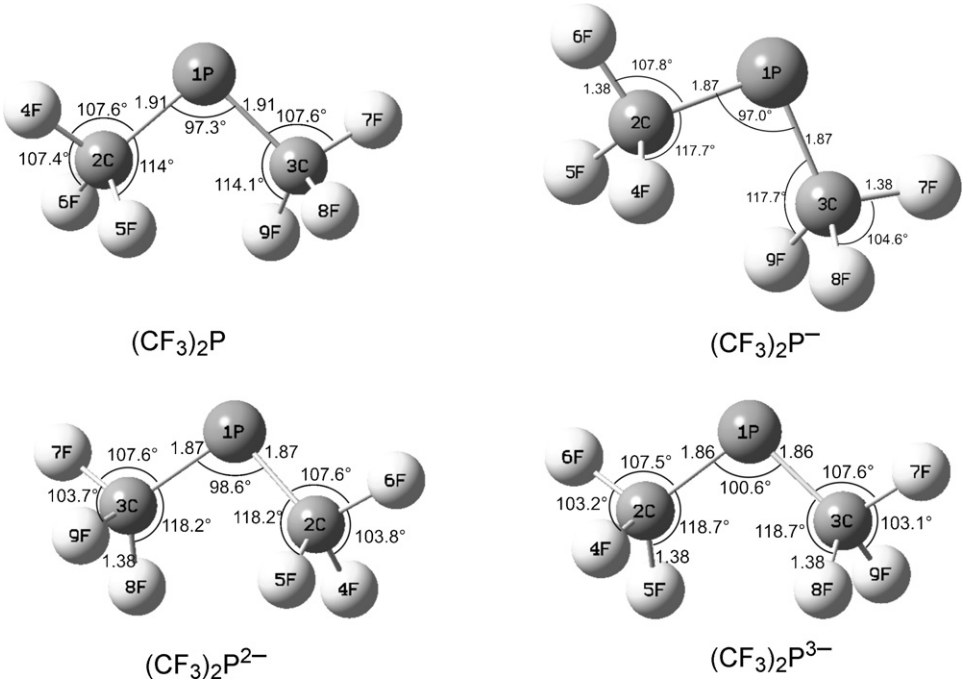

Fig. 4. Optimized structures of $(CF_3)_2P$ neutral and anions. Angles in degrees and bond lengths are in Angstrom.

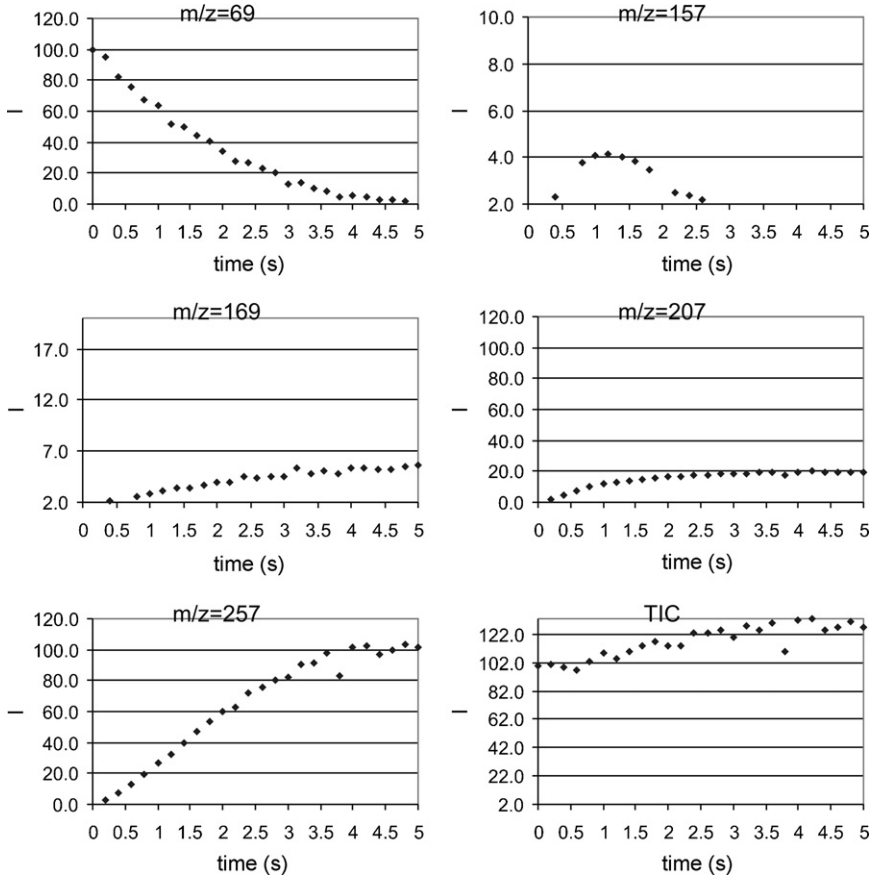

Fig. 5. Time dependent signal intensities of all observed ions during an ion–molecule reaction between CF_3^- and the neutrals at 2×10^{-7} mbar. TIC is the sum of all signal intensities of observed ions.

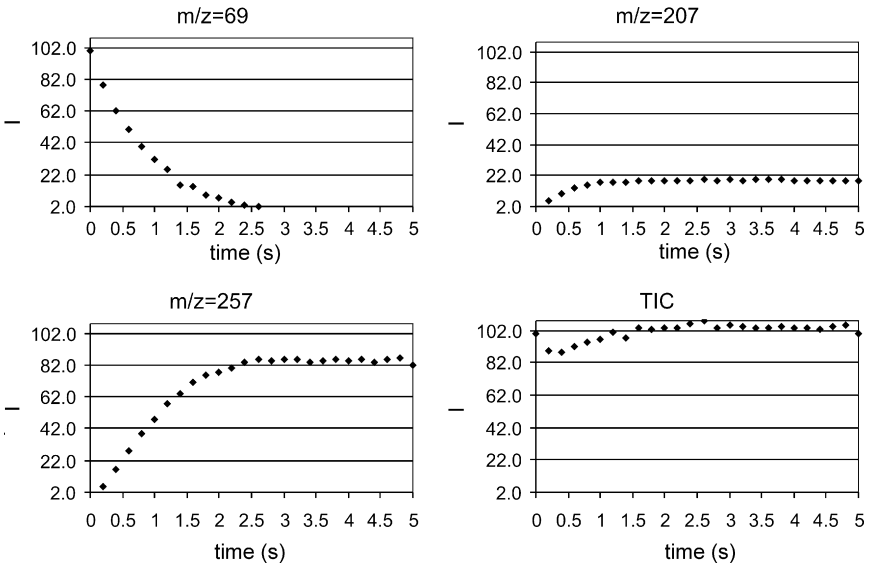

Fig. 6. Ion–molecule reactions between CF_3^- and the neutrals at 2×10^{-7} mbar. The tertiary ion $m/z = 157$ has been continuously quenched during the entire reaction time. TIC is the sum of all signal intensities of observed ions.

there is no route for a nucleophic addition of CF_3^- toward any carbon or fluoride atom in the three CF_3 groups available in $(CF_3)_3P$ along the potential energy surface of the reaction system CF_3^- and $(CF_3)_3P$. Furthermore, Mulliken charge distribution reinforces this fact, since the three F-atoms in the CF_3^- group as well as the F-atoms in all three CF_3 groups in $(CF_3)_3P$ have relatively high negative charge values (see Fig. 7). This leads to mutual coulombic repulsion between the negative partial charges of both CF_3^- and the substrate. There might be an approach of one F-atom in CF_3^- toward the electrophilic carbon center of one of the three CF_3 groups in $(CF_3)_3P$, since there is a large charge difference between them. However, steric hindrance produced by these two reaction partners, that are heavily crowded with negatively charged F-atoms, combined with their large coulombic repulsion makes this approach inapplicable.

The only route, that has been found using DFT calculations, is a nucleophilic addition of the CF_3^- anion on the phosphorous atom in $(CF_3)_3P$, Fig. 8. The energy of this association complex has been found to be −11.5 kcal/mol (298 K), if one of the F-atoms of CF_3^- is added directly to the phosphorous atom of $(CF_3)_3P$. This complex leads to the observed $(CF_3)_3PF^-$ ($m/z = 257$) after release of a CF_2 molecule.

For the formation of $(CF_3)_4P^-$ a different association complex is necessary. The carbon atom and not one fluorine atom of CF_3^- has to associate directly with the phosphorous atom of $(CF_3)_3P$. The resultant anion $(CF_3)_4P^-$ lies 33.1 kcal/mol (298 K) below the sum of the energies of the reactants, CF_3^- and $(CF_3)_3P$. However, this anion has not been experimentally observed in ICR in the pressure range from 2×10^{-7} mbar to 8×10^{-6} mbar. This ion has a very short life time in the gas phase. It cannot be stabilized by collisions in this pressure range. Higher pressures are not applicable in ICR, since peak broadening and loss of ions occur. The energy of −33.1 kcal/mol released by formation of $(CF_3)_4P^-$ can induce a rearrangement producing $(CF_3)_2PF_2^-$ ($m/z = 207$), that has been experimentally observed in ICR as a major product ion, after release of C_2F_4 fragment. The calculated gas phase structures of $(CF_3)_4P^-$ and $(CF_3)_3PF\_CF_2^-$ are shown in Fig. 8.

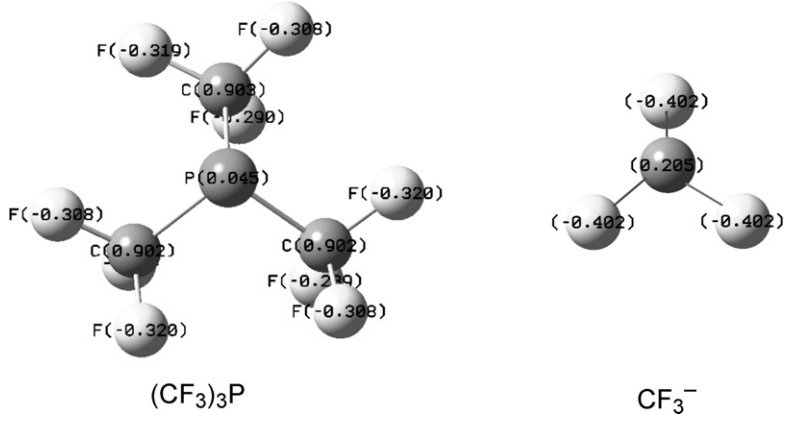

Fig. 7. Mulliken charge distribution in $(CF_3)_3P$ neutral and CF_3^- ion.

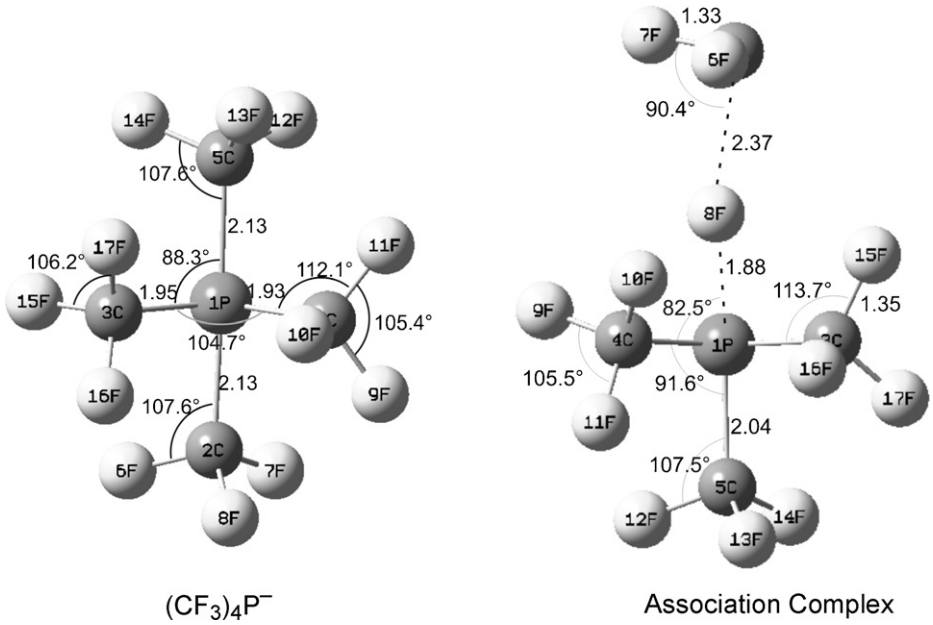

Fig. 8. Gas phase structures for $(CF_3)_4P^-$ and the association complex $(CF_3)_3PF\_CF_2^-$.

Self-CID experiments on the product ions of the ion–molecule reaction between CF_3^- and the neutrals support the identity of the discussed product ions.

The fragmentation pattern of the product ion $m/z = 157$ contains CF_3^- (10.2%) only after 50 ms of delay time. Both F^- (11.2%) and CF_3^- (13.3%) were observed after 100 ms delay time of acceleration. Fragmentation pattern of the product ion $m/z = 169$ produces CF_3^- (6.2%) only after 100 ms.

Acceleration of the product ion $m/z = 207$ produces CF_3^- (5.5%) after 50 ms and both F^- (4.4%) and CF_3^- (6.1%) after 100 ms, whereas $m/z = 257$ acceleration produces CF_3^- (12.7%) only after 50 ms.

Ion–molecule reactions of CF_3^- lead to the formation of the three major product ions $(CF_3)_3PF^-$ ($m/z = 257$), $(CF_3)_2PF_2^-$ ($m/z = 207$), and $CF_3PF_3^-$ ($m/z = 157$) in exothermic reactions (Eq. 6.1, 6.2, and 6.3) (Scheme 4).

3.2.6. A final word about self-CID of secondary ion $m/z = 157$

The product ion $m/z = 257$ has been observed as a result of an energetic ion–molecule reaction between the accelerated secondary ion $CF_3PF_3^-$ $m/z = 157$ and the neutral molecules (as shown in self-CID experiment of $CF_3PF_3^-$ ($m/z = 157$) in Section 3.2.3. The ion–molecule reaction between $CF_3PF_3^-$ ($m/z = 157$) and the neutrals leading to $(CF_3)_3PF^-$ ($m/z = 257$) is slightly endothermic, while the production of $(CF_3)_2P–PF_3^-$ ($m/z = 257$) from the same reaction system is highly exothermic. Thus, energy supply is needed to produce the phosphoranide $(CF_3)_3PF^-$ and this is exactly what was provided in the self-CID experiment through accelerating of the secondary ion $CF_3PF_3^-$.

On the other hand, the tertiary ion $CF_3PF_3^-$ ($m/z = 157$) formed in the thermal ion–molecule reaction between CF_3^- and the neutral molecules produces only a small proportion of the phosphoranide $(CF_3)_3PF^-$ ($m/z = 257$) as a quaternary product ion. The high resolution measurement of the product ion $m/z = 257$ formed from the same ion–molecule reaction proves the phosphoranide structure $(CF_3)_3PF^-$.

In Eq. (5.2), we have shown, that formation of $(CF_3)_2P–PF_3^-$ ($m/z = 257$) from $CF_3PF_3^-$ ($m/z = 157$) is exothermic. We conclude, that the absence of $(CF_3)_2P–PF_3^-$ ($m/z = 257$) is due to the chemical nature of this structure which has very high electron-

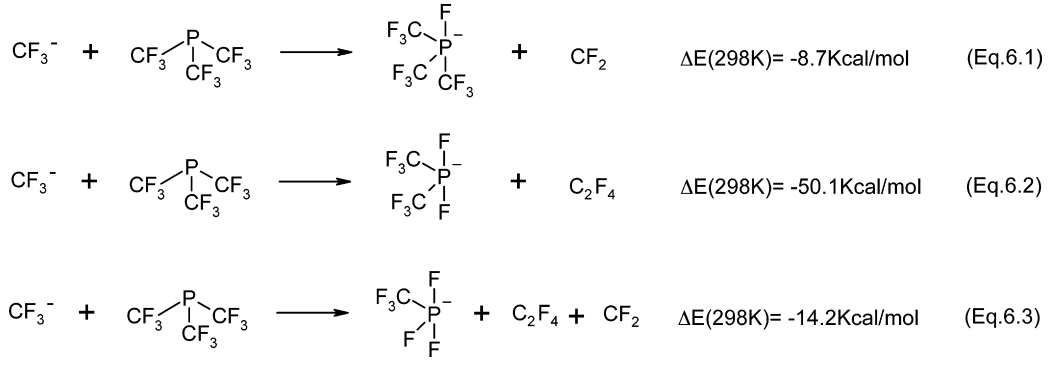

Scheme 4. Ion-neutral reactions between CF_3^- and $(CF_3)_3P$.

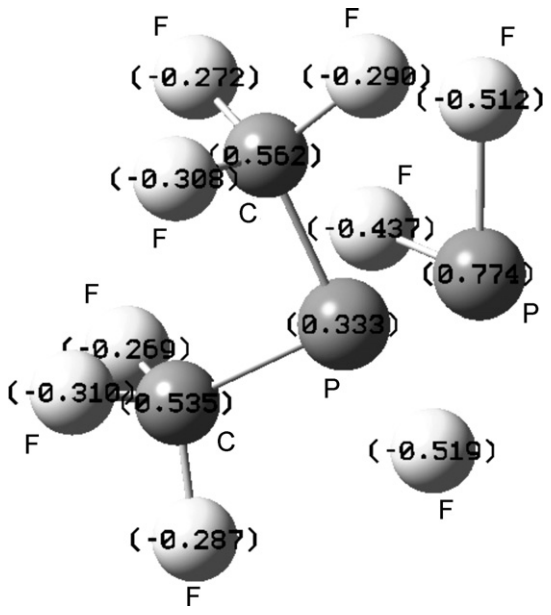

Fig. 9. Mulliken charge distribution of $(CF_3)_2P–PF_3^-$ phosphoranide ion.

withdrawing groups that remove the required electron density for the P–P bond formation. Fig. 9 shows the DFT calculated Mulliken charge distribution of the $(CF_3)_2P–PF_3^-$ phosphoranide ion. It is clear to note that both two phosphorus atoms as well as both carbon atoms of the two CF_3 groups bear large partial positive charges. From these obvious partial positive charges on both phosphorus atoms, it can be concluded, that there is too little electron density on the central line connecting these two phosphorus atoms in this ion.

3.2.7. Conclusion

Two sources, $(CF_3)_2P^-$ ($m/z = 169$) and CF_3^- ($m/z = 69$) have been experimentally identified for the production of the phosphoranides $(CF_3)_3PF^-$ ($m/z = 257$), $(CF_3)_2PF_2^-$ ($m/z = 207$), and $CF_3PF_3^-$ (m/z157) in the gas phase at 2×10^{-7} mbar. It is shown that these phosphoranides are formed in large yields in a reaction time of 1 s, if the primary phosphide ion $(CF_3)_2P^-$ ($m/z = 169$) is accelerated. However, phosphoranide formation requires a relatively high pressure (2×10^{-7} mbar). DFT calculations for the adiabatic electron affinity clearly shows that multiply charged anions of the phosphide do not exist at these experimental conditions. Gas phase structures of several phosphide and phosphoranide anions have been calculated and discussed in this article.

The phosphoranide $(CF_3)_4P^-$ ($m/z = 307$) was not observed experimentally in the gas phase. The association complex between CF_3^- and $(CF_3)_3P$ shows a fluorine phosphorus interaction. Its formation is exothermic by 11.5 kcal/mol. This complex dissociates to the observed $(CF_3)_3PF^-$ ($m/z = 257$) and difluorocarbene.

Acknowledgements

B. Kanawati thanks the FCI (Fonds der Chemischen Industrie) for a PhD grant. We would like to thank Dr. M. Bremer for some of the DFT calculations presented in this paper, and Prof. Dr. G.-V. Röschentaler, O. Shyshkov, and Dr. A. Kolomeitsev for a sample of tris(trifluoromethyl)phosphine.

Appendix A. Supplementary data

Tables of accurate mass measurements and fragmentation patterns as well as diagrams for the ejection experiments are provided as supplementary material.

Supplementary data associated with this article can be found, in the online version, at doi:10.1016/j.ijms.2007.04.008.

References

[1] A.B. Burg, Inorgan. Chem. 25 (1986) 4751.
[2] A.B. Burg, I.H. Sabherwal, Inorgan. Chem. 9 (1970) 974.
[3] H.G. Ang, S.G. Ang, S.W. Du, J. Organometal. Chem. 590 (1) (1999) 1.
[4] H.G. Ang, S.G. Ang, S.W. Du, J. Chem. Soc. Dal. Trans. 16 (1999) 2799.
[5] H.G. Ang, S.G. Ang, S.W. Du, Phosphor. Sulfur Sil. Relat. Elements 111 (1–4) (1996), p. 683.
[6] J.A.S. Howell, N. Fey, J.D. Lovatt, J. Chem. Soc. Dal. Trans. 17 (1999) 3015.
[7] J.A.S. Howell, J.D. Lovatt, P. McArdle, Inorgan. Chem. Commun. 1 (3) (1998) 118.
[8] A. Tworowska, I. Dabkowski, W. Michalski, J. Angewandte Chemie 113 (2001) 2982;
G.-V. Röschenthaler, Bissky FG., A.A. Kolomeitsev, J. Fluor. Chem. 79 (1) (1996) 103.
[9] L.J. Krause, J.A. Morrison, J. Am. Chem. Soc. 103 (1981) 2995.
[10] G.-V. Röschentaler, O. Shyshkov, Ph.D. Thesis, University of Bremen, 2006.
[11] A. Kolomeitsev, M. Görg, U. Dieckbreder, E. Lork, G.-V. Röschenthaler, Phosphor. Sulf. Silic. 109 (1996) 597.
[12] K.B. Dillon, Chem. Rev. 94 (1994) 1441.
[13] M. Allemann, Hp. Kellerhals, K.P. Wanczek, Chem. Phys. Lett. 75 (1980) 328.
[14] N. Tobias, Diploma Thesis, University of Bremen, Germany, September, 2000.
[15] D.A. Dahl, Idaho National Engineering and Environmental Laboratory, Idaho Falls, ID 83415.
[16] M.J. Frisch, G.W. Trucks, H.B. Schlegel, G.E. Scuseria, M.A. Robb, J.R. Cheeseman, J.A. Montgomery Jr., T. Vreven, K.N. Kudin, J.C. Burant, J.M. Millam, S.S. Iyengar, J. Tomasi, V. Barone, B. Mennucci, M. Cossi, G. Scalmani, N. Rega, G.A. Petersson, H. Nakatsuji, M. Hada, M. Ehara, K. Toyota, R. Fukuda, J. Hasegawa, M. Ishida, T. Nakajima, Y. Honda, O. Kitao, H. Nakai, M. Klene, X. Li, J.E. Knox, H.P. Hratchian, J.B. Cross, V. Bakken, C. Adamo, J. Jaramillo, R. Gomperts, R.E. Stratmann, O. Yazyev, A.J. Austin, R. Cammi, C. Pomelli, J.W. Ochterski, P.Y. Ayala, K. Morokuma, G.A. Voth, P. Salvador, J.J. Dannenberg, V.G. Zakrzewski, S. Dapprich, A.D. Daniels, M.C. Strain, O. Farkas, D.K. Malick, A.D. Rabuck, K. Raghavachari, J.B. Foresman, J.V. Ortiz, Q. Cui, A.G. Baboul, S. Clifford, J. Cioslowski, B.B. Stefanov, G. Liu, A. Liashenko, P. Piskorz, I. Komaromi, R.L. Martin, D.J. Fox, T. Keith, M.A. Al-Laham, C.Y. Peng, A. Nanayakkara, M. Challacombe, P.M.W. Gill, B. Johnson, W. Chen, M.W. Wong, C. Gonzalez, J.A. Pople, Gaussian 03, Revision C. 02, Gaussian, Inc., Wallingford, CT, 2004.
[17] B. Kanawati, Diploma Thesis, University of Bremen, Germany, September, 2003.
[18] B. Hoge, C. Thösen, Inorgan. Chem. 40 (2001) 3113.
[19] B. Hoge, C. Thösen, T. Herrmann, Inorgan. Chem. 42 (2003) 3633.
[20] J.C. Kleingeld, N.M.M. Nibbering, Lectures Notes in Chemistry 31; Ion Cyclotron Resonance Mass Spectrometry II, Springer-Verlag, Berlin, 1982, pp. 209–228.